

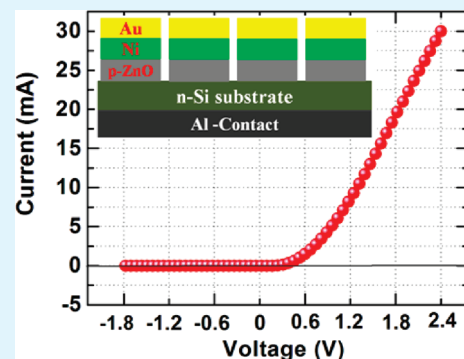
A Codoping Route to Realize Low Resistive and Stable p-Type Conduction in (Li, Ni):ZnO Thin Films Grown by Pulsed Laser Deposition

E. Senthil Kumar,[†] Jyotirmoy Chatterjee,[‡] N. Rama,[†] Nandita DasGupta,[‡] and M. S. Ramachandra Rao^{*,†}

[†]Department of Physics, Nano Functional Materials Technology Centre, Materials Science Research Centre and [‡]Department of Electrical Engineering, Microelectronics & MEMS Laboratory, Indian Institute of Technology Madras, Chennai–600036, India

ABSTRACT: We report on the growth of Li–Ni codoped p-type ZnO thin films using pulsed laser deposition. Two mole percent Li monodoped ZnO film shows highly insulating behavior. However, a spectacular decrease in electrical resistivity, from 3.6×10^3 to $0.15 \Omega \text{ cm}$, is observed by incorporating 2 mol % of Ni in the Li-doped ZnO film. Moreover, the activation energy drops to 6 meV from 78 meV with Ni incorporation in Li:ZnO lattice. The codoped [ZnO:(Li, Ni)] thin film shows p-type conduction with room temperature hole concentration of $3.2 \times 10^{17} \text{ cm}^{-3}$. Photo-Hall measurements show that the Li–Ni codoped p-ZnO film is highly stable even with UV illumination. XPS measurements reveal that most favorable chemical state of Ni is Ni^{3+} in (Li, Ni): ZnO. We argue that these Ni^{3+} ions act as reactive donors and increase the Li solubility limit. Codoping of Li, with other transitional metal ions (Mn, Co, etc.) in place of Ni could be the key to realize hole-dominated conductivity in ZnO to envisage ZnO-based homoepitaxial devices.

KEYWORDS: ZnO, resistivity, codoping, II–VI semiconductors, doping studies



INTRODUCTION

ZnO has always been considered as one of the most promising material candidates for ultraviolet light emitting diodes and laser diodes because of its direct wide band gap ($\sim 3.37 \text{ eV}$) and relatively large exciton binding energy (60 meV), compared with that of GaN (25 meV) and ZnSe (22 meV), at room temperature.¹ The successful demonstration of room-temperature electroluminescence from ZnO-based homo- and heterojunctions have proved that the material is ideal for next generation short wavelength optoelectronic devices.^{2–5} Recent studies on the growth of p-type ZnO resolve the long existing problem of doping asymmetry in ZnO and the stability of p-type conductivity.^{6–8} All possible p-type dopants, such as group V elements [N, P, As, Sb] and group I and IB elements [Li, Na, K, Ag, Cu], have been tried to realize p-type conduction and UV-electroluminescence in ZnO.^{9–13} Few attempts have been made to realize the lasing action in ZnO-based p–n junctions and multiquantum wells.^{14,15} Nitrogen substitution at the oxygen site in ZnO appears to be promising for p-type conduction and many groups have reported room-temperature electroluminescence from N-doped ZnO-based homojunctions.^{2,3} P, As, and Sb seem to be good candidates for p-type dopants. Among group I elements, theoretically, Li possesses shallow acceptor levels.¹⁶ However, no electroluminescence is achieved from Li-substituted (Li_{Zn}) ZnO-based homojunctions. Contrary to theoretical prediction, it was observed experimentally that Li doping in ZnO increases the resistivity drastically by several orders and makes it insulating. This is because Li being a small ion can easily occupy the interstitial positions (Li_i) rather than the substitutional sites. Thus stabilizing the Li-ion in the ZnO lattice as an acceptor

dopant and the growth of low resistive and stable p-type ZnO still remains a challenging problem.

The donor–acceptor codoping method is believed to be promising, because it will enhance the acceptor solubility limit and raise the acceptor to shallow level.¹⁷ Lee et al. have suggested that codoping Li with H will be ideal for getting low resistive p-ZnO.¹⁸ However, formation of complexes such as $\text{Li}_{\text{Zn}}-\text{Li}_i$, $\text{Li}_{\text{Zn}}-\text{H}$, and $\text{Li}_{\text{Zn}}-\text{AX}$ will limit the p-type doping concentration.¹⁹ Zeng et al. have reported a low resistivity of $16.4 \Omega \text{ cm}$ with a Hall mobility of $2.65 \text{ cm}^2 \text{ V}^{-1} \text{ s}^{-1}$ by Li monodoping.²⁰ The same group has tried Li–N dual-acceptor doping in ZnO (ZnO: Li-N) and achieved a low resistivity of $0.93 \Omega \text{ cm}$ and a Hall mobility of $0.75 \text{ cm}^2 \text{ V}^{-1} \text{ s}^{-1}$ with acceptor activation energy of 95 meV.²¹ Recently, our group has reported a dramatic decrease in the bulk resistivity of Ni doped ZnO.²² This was attributed to the impurity d-band splitting of Ni ion in the tetrahedral crystal field of ZnO. Recent experimental and theoretical reports show that incorporation of Li in transition metal (TM) ion doped ZnO will stabilize the ferromagnetic ordering thereby increase the Curie temperature.^{23,24} However, what happens to the stability of p-type conduction when a TM ion is incorporated in Li-doped ZnO lattice, remains to be seen. This question has motivated us to examine the codoping of Li–Ni to achieve a stable and low resistive p-type ZnO. To the best of our knowledge, no report is published on Li–Ni-codoped p-ZnO thin films. In this letter, we report on the growth of Li–Ni codoping in ZnO and demonstrate that the system is promising to achieve highly stable and low resistive p-ZnO.

Received: February 15, 2011

Accepted: May 20, 2011

Published: May 20, 2011

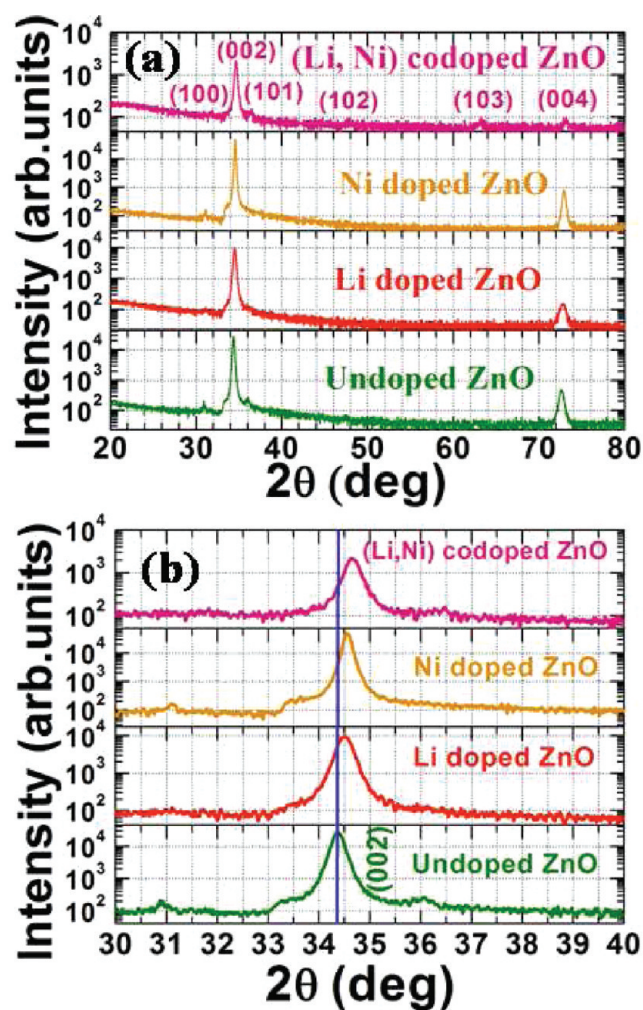


Figure 1. (a) XRD patterns of undoped, Li-doped, Ni-doped, and Li–Ni-codoped ZnO thin films, (b) magnified (002) ZnO peaks of undoped and doped ZnO thin films.

EXPERIMENTAL DETAILS

ZnO, $Zn_{1-x}Li_xO$, $Zn_{1-y}Ni_yO$ and $Zn_{1-x-y}Li_xNi_yO$ ($x = 0.02$ and $y = 0.02$) thin films were grown by pulsed laser deposition (PLD) technique. PLD targets were prepared using conventional solid state reaction method. Li-doped, Ni-doped, and Li–Ni-codoped ZnO powders were synthesized by mixing stoichiometric amounts of ZnO, NiO, and Li_2CO_3 . Initially the powders were ground for 1 h, heated at 750 °C for 12 h, and then pressed into 12 mm diameter pellets and sintered at 900 °C for 12 h. Quartz substrates were used for the growth after cleaning them by ultrasonic cleaner using ethanol, acetone, and deionized water. 300 nm thick films were grown at a substrate temperature of 400 °C with O_2 partial pressure of 0.15 mbar. Crystalline nature of the ZnO films was analyzed by X-ray diffractometer (XRD) (PANalytical, XPERT-pro) using $Cu K\alpha$ radiation. Electrical resistivity, carrier concentration, and mobility of the ZnO films were measured by Physical Property Measurement System (PPMS, Quantum Design). Indium contacts were used for both Hall effect and electrical resistivity measurements with Van der Pauw configuration. Photo-Hall measurements were performed with the same contacts and geometry of that of ordinary (no UV exposure) Hall measurements. Li–Ni codoped ZnO thin film was exposed to UV light of $12 \mu W$ (365 nm) for a fixed time (e.g., 10 min) and then Hall measurements were performed. This was repeated for longer UV exposure times like 20 min, 30 min, etc. Carrier concentrations

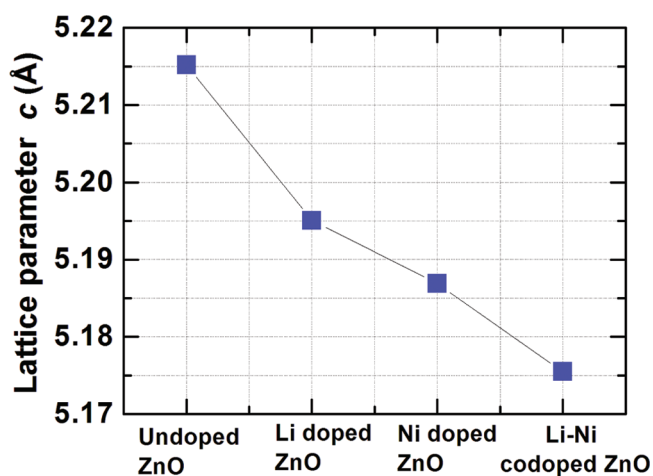


Figure 2. *c*-Lattice parameter of the undoped, Li-doped, Ni-doped, and Li–Ni-codoped ZnO thin films.

Table 1. Room-Temperature Electrical Transport Properties of Li-Doped, Ni-Doped, and Li–Ni-Co-doped ZnO Thin Films

sample	carrier type	resistivity (Ω cm)	carrier concentration (cm^{-3})	activation energy (meV)
Li-doped ZnO		3.6×10^3		78
Ni-doped ZnO	n	0.21	3.1×10^{17}	11
Li–Ni-codoped ZnO	p	0.15	3.2×10^{17}	6

of all the films were calculated using the Hall coefficient that was measured at a magnetic field strength of 7 T. For Li-doped ZnO, electrical resistivity measurement was carried out using liquid nitrogen as cryogene. X-ray photoelectron spectroscopy (XPS) measurements were performed using PHI Versa Probe (Physical electronics, USA).

RESULTS AND DISCUSSION

X-ray diffraction patterns reveal that the films are predominantly oriented in (002) direction of the wurtzite hexagonal structure (Figure 1a). However, the presence of minor (100) and (101) peaks show that the films are polycrystalline in nature, which may be due to the amorphous nature of the quartz substrate. No trace of any secondary phases is found in the films. The ionic radii of Li, Ni, and Zn in the tetrahedral coordination are 0.59, 0.69, and 0.74 Å, respectively. Hence when the smaller ions are substituted in place of Zn, XRD peaks shift toward higher 2θ values, which is clearly seen in the Figure 1b. Figure 2 shows the variation of the *c*-lattice parameter with the addition of Li and Ni to ZnO lattice. The value of *c* for the undoped ZnO is 5.215 Å, which is found to decrease for all the doped films (Li monodoped, 5.195 Å; and Li–Ni codoped, 5.176 Å). This clearly indicates the incorporation of Li and Ni in to the ZnO lattice.

Table 1 gives a summary of parameters obtained from electrical transport study on Li-monodoped, Ni-monodoped, and Li–Ni-codoped ZnO thin films. Room-temperature electrical transport measurements show that 2 mol % of Li-monodoped ZnO thin film is highly resistive in nature with a resistivity of $3.6 \times 10^3 \Omega$ cm. Zeng et al. have reported that above 0.5 at % of Li doping in ZnO leads to a very high resistivity of about 1×10^3 to $1 \times 10^4 \Omega$ cm.²⁰

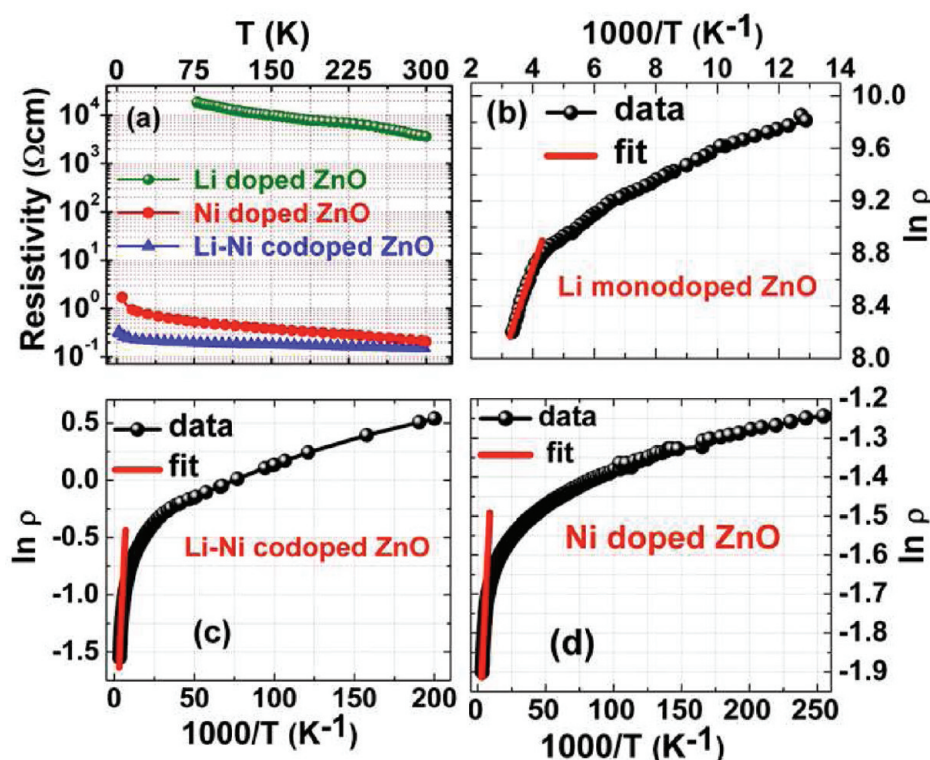


Figure 3. (a) Temperature-dependent electrical resistivity and (b–d) $\ln(\rho)$ vs $1/T$ fits of the Li-doped, Li–Ni-doped, and Ni-codoped ZnO thin films.

To overcome this doping limitation, we codoped 2 mol % of Ni with Li in ZnO. For comparison, 2 mol % of Ni-monodoped ZnO thin film also was grown at the same condition. Ni monodoped ZnO thin film shows resistivity $\sim 0.21 \Omega \text{ cm}$, whereas room-temperature resistivity of Li–Ni-codoped ZnO thin film is $\sim 0.15 \Omega \text{ cm}$, which is 4 orders of magnitude less compared with Li-monodoped ZnO thin film. Figure 3a shows the temperature dependent electrical resistivity of the Li-monodoped, Ni-monodoped, and Li–Ni-codoped ZnO thin films. Figures 3b–d show the Arrhenius curve fits, $\ln(\rho)$ versus $1/T$, of the thermally activated band conduction mechanism of Li-monodoped, Li–Ni-codoped and Ni-monodoped ZnO thin films. From the $\ln(\rho)$ versus $1/T$ plots, we have calculated the activation energy of these three films. Li-monodoped ZnO thin film shows activation energy of 78 meV, and the activation energy drops to 6 meV for Li–Ni-codoped ZnO thin film. Ni-monodoped ZnO thin film shows activation energy of ~ 10 meV. These values clearly reveal that incorporation of Ni in Li: ZnO lattice increases the conductivity by several orders. Because of high resistivity, Hall effect measurements could not be carried out on Li-monodoped ZnO thin film. Ni-monodoped ZnO thin film shows n-type conductivity with an electron concentration of $3.1 \times 10^{17} \text{ cm}^{-3}$ and a mobility of $\sim 96 \text{ cm}^2 \text{ V}^{-1} \text{ s}^{-1}$, whereas Li–Ni-codoped ZnO thin film exhibits a stable p-type conductivity with a hole concentration of $3.2 \times 10^{17} \text{ cm}^{-3}$ and a high mobility of $130 \text{ cm}^2 \text{ V}^{-1} \text{ s}^{-1}$. It is known that confirming p-type conduction in ZnO-based thin films is a difficult problem, and hence in addition to finding the sign of the Hall coefficient, we have carried out magnetic field variation (from 0 to 7 T) of the Hall voltage for the Ni doped and Li–Ni codoped ZnO thin films. It is very clear from Figure 4 that the linear plot of V_{xy} as a function of applied magnetic field (B) for

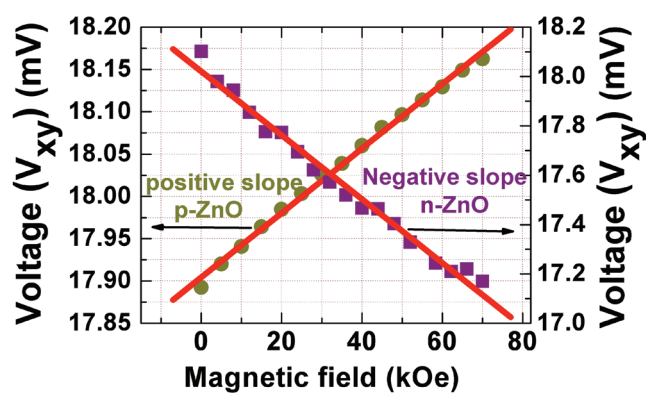


Figure 4. Variation in transverse voltage (V_{xy}) with magnetic field for Ni-doped (n-type) and Li–Ni-codoped (p-type) ZnO thin films.

Li–Ni-codoped ZnO thin film shows positive slope that is a clear indication of p-type conduction. However, Ni-doped ZnO shows negative slope as expected for n-type conduction. Li–Ni-codoped ZnO thin film shows relatively high mobility compared with the reported values for Li-doped ZnO thin films. Similar values of high mobility were observed by Bian et al. and others in N–In- and N–Al-codoped p-ZnO thin films.^{25,26} They have shown a maximum mobility of $166 \text{ cm}^2 \text{ V}^{-1} \text{ s}^{-1}$ with a low resistivity, $9 \times 10^{-3} \Omega \text{ cm}$. Moreover such high hole mobility values were reported even for the wide band gap p-GaN thin films.^{27,28} Very recently, Samanta et al. have shown a room-temperature mobility of $57.44 \text{ cm}^2 \text{ V}^{-1} \text{ s}^{-1}$ for PLD-grown Sb-doped ZnO thin films.²⁹ Wang et al. have reported p-type conduction in undoped polycrystalline ZnO thin films with high Hall mobility of

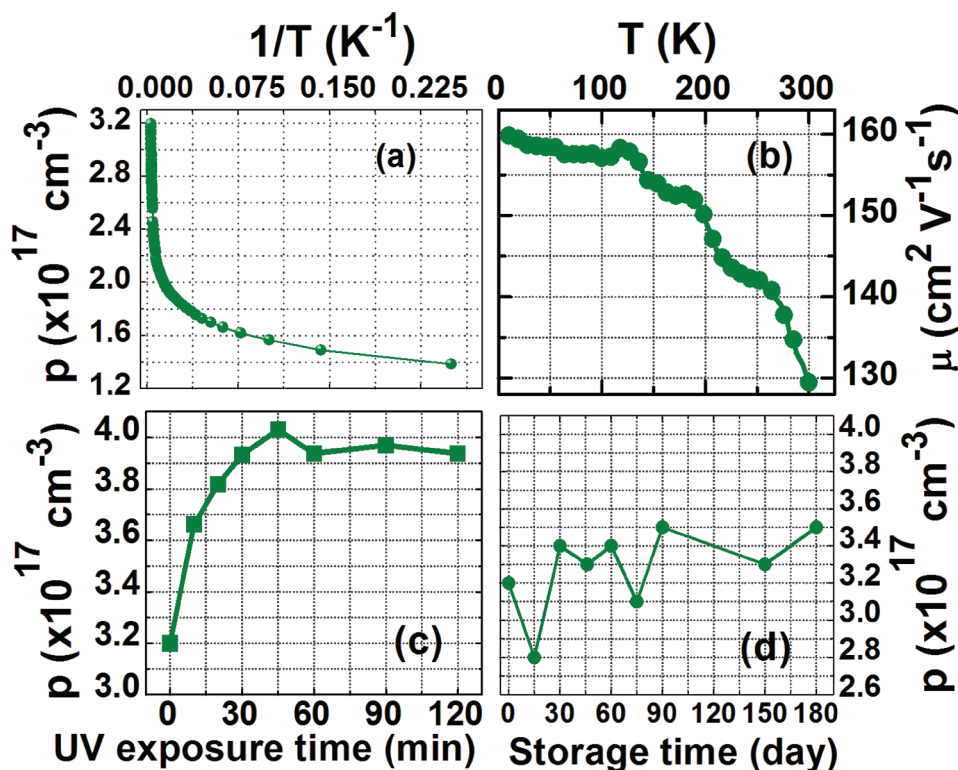


Figure 5. (a) Temperature dependence of hole concentration, (b) temperature variation of the mobility, (c) hole concentration with UV exposure time, and (d) hole concentration as a function of the storage time after deposition of the Li–Ni-codoped ZnO thin film.

$261 \text{ cm}^2 \text{V}^{-1} \text{s}^{-1}$.³⁰ This was attributed to the formation of quasi-two-dimensional hole gas (2DHG) at the grain boundaries of the polycrystalline thin film. In our present study, our Li–Ni-codoped ZnO is also a polycrystalline thin film and hence there is a possibility of formation of the 2DHG at the grain boundaries that may lead to high carrier mobility.

Panels a and b in Figure 5 show the temperature-dependent Hall (T-Hall) measurements of Li–Ni-codoped ZnO thin film. The film shows stable p-type conductivity for the complete temperature range (300–5 K) indicating holes are the only major carriers in the system. The mobility increases with decrease in temperature and a maximum value of $160 \text{ cm}^2 \text{V}^{-1} \text{s}^{-1}$ is observed at 5 K. To examine the stability of p-type conduction, we performed Hall measurements by illuminating the p-ZnO thin film with UV-light ($\lambda = 365 \text{ nm}$) of $12 \mu\text{W}$ power. Figure 5c gives the hole concentration at different UV exposure times. Interestingly we observed that the p-type conductivity is highly stable even with 120 min of UV exposure time. Moreover, the hole concentration slightly increases with UV illumination and saturates at 40 min of exposure time and remains the same up to 120 min of UV exposure. This is in agreement with Yao et al. report, which shows that nitrogen doped n-ZnO thin film turns to p-ZnO by irradiating several times with sun light and remains p-type.³¹ However some reports show that p-ZnO reverts to n-ZnO upon illuminating with UV irradiation.³² Figure 5d gives the hole concentration with time after deposition. Over a span of 180 days, several Hall measurements were carried out to examine the stability of p-type conduction with time. The measurement results show that the film retains its p-type behavior even after 180 days of storage with almost the same hole concentration as on

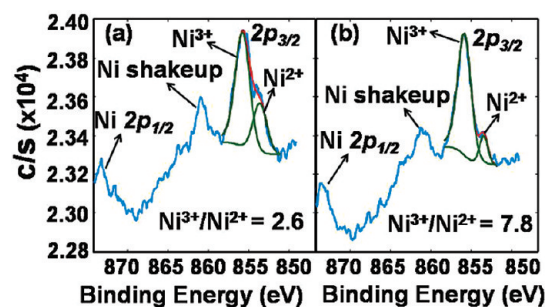


Figure 6. X-ray photoelectron spectra of Li-doped, Ni-doped, and Li–Ni-codoped ZnO thin films. (a) Ni 2p levels of Ni-doped ZnO thin film and (b) Ni 2p levels of Li–Ni-codoped ZnO thin films.

the day of deposition. This result clearly indicates that the p-type conduction in Li–Ni-codoped ZnO thin film is highly stable.

It is interesting to note that Li–Ni-codoped p-ZnO thin film exhibits a low resistivity of $0.15 \Omega \text{ cm}$, while comparing with Li-doped ZnO and dual-acceptor doped p-ZnO: Li–N system.²¹ How does an isovalent (Ni^{2+}) doped Li:ZnO thin film shows a low resistive, high mobility, and stable p-type conduction? The origin of low resistivity and high p-type conductivity can be understood as follows: On the basis of theoretical calculations, Pei et al. have reported that when Li and Ni is codoped in ZnO, Li tends to substitute the sites near Ni ions.²⁴ Petit et al. have shown that when a transition metal (TM) alone is doped in ZnO a stable TM^{2+} configuration is favored, whereas, TM^{3+} configuration is favored when an additional hole is introduced in to the ZnO lattice.³³ Thus in a Li–Ni-codoped ZnO system, Li is likely to be

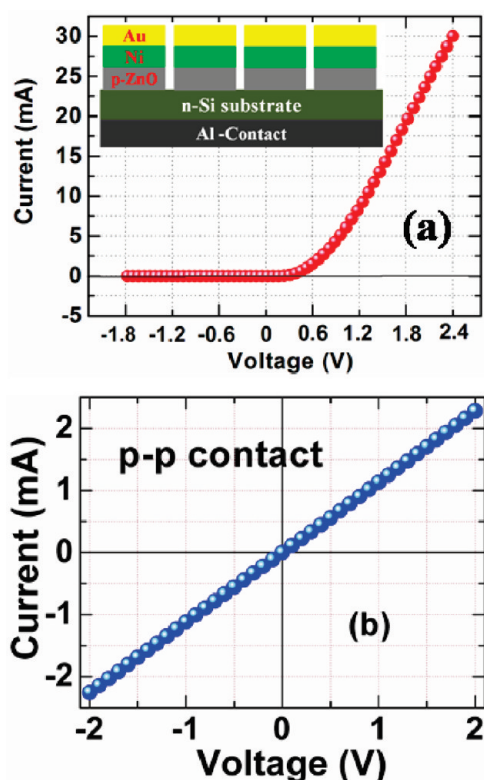


Figure 7. (a) Current–voltage (I – V) characteristics of the p-ZnO/n-Si junction diode and the inset shows the schematic of the p–n junction device and (b) I – V characteristics of the Ni/Au contacts on p-ZnO layer.

the nearest site of Ni ion and hence promotes Ni^{2+} into Ni^{3+} . To verify this theory, we have performed XPS measurements on Li-doped, Ni-doped, and Li–Ni-codoped ZnO thin films. Panels a and b in Figure 6 show the Ni 2p levels of Ni-doped and Li–Ni-codoped ZnO thin films. For 2 mol % of Ni-doped ZnO thin film, Ni 2p_{3/2} level consists of two peaks centered around 853.63 and 855.74 eV corresponding to Ni^{2+} and Ni^{3+} chemical states, respectively. The area ratio ($\text{Ni}^{3+}/\text{Ni}^{2+}$) of the Ni^{3+} and Ni^{2+} ion is found to be 2.6. For Li–Ni-codoped ZnO thin film, peaks corresponding to Ni^{2+} and Ni^{3+} chemical states are centered at 853.49 and 855.85 eV, respectively. The area ratio of $\text{Ni}^{3+}/\text{Ni}^{2+}$ ion for this codoped system is 7.8. This reveals that the concentration of Ni^{3+} ion increases in Li–Ni codoped ZnO, when compared with that of Ni-doped ZnO, when Li^+ ions are added and clearly indicates that in the Li–Ni codoped ZnO system, the most favorable chemical state of Ni ion is Ni^{3+} . As reported by Yamamoto et al. this Ni^{3+} ion will act as a reactive donor like Al in Li–Al-codoped ZnO and form $\text{Li}^+ - \text{Ni}^{3+} - \text{Li}^+$ (acceptor–donor–acceptor) complexes, which are responsible for p-type conductivity.¹⁷ This reactive donor (Ni^{3+}) will increase the Li solubility limit and raises acceptor (Li) into a shallow level. This is the reason why Li–Ni codoped ZnO thin film shows low resistivity when compared with Li doped ZnO and dual-acceptor doped p-ZnO:Li–N thin films.

To further verify the p-type conductivity of Li–Ni-codoped ZnO thin films, we have fabricated p-ZnO/n-Si heterojunction diodes to demonstrate the rectifying current–voltage (I – V) characteristics. The junction area was defined as $300 \mu\text{m} \times 300 \mu\text{m}$

using standard optical lithography technique. For ohmic contacts, Ni/Au and Al were deposited by e-beam and thermal evaporation techniques on p-ZnO and n-Si, respectively. Figure 7a shows the room temperature (300 K) I – V characteristics of the heterojunction diode. The diode shows a typical rectifying behavior, with a turn on voltage of 0.8 V. This study further confirms p-type conduction in Li–Ni-codoped ZnO thin films. Figure 7(b) shows the I – V characteristics between two Ni/Au contact pads on p-ZnO layer. The linear I – V curves confirm that the contact is ohmic. Thus, it can be concluded that the rectifying nature of the diode is indeed due to p-ZnO/n-Si interface and not to any Schottky barrier formed at the metal/ZnO interface.

CONCLUSIONS

In summary, a method has been proposed to realize highly stable and low resistive p-ZnO thin film by codoping with Li and Ni. Using this method, a low resistivity of $0.15 \Omega \text{ cm}$ with a hole concentration of $3.2 \times 10^{17} \text{ cm}^{-3}$ and a mobility of $130 \text{ cm}^2 \text{ V}^{-1} \text{ s}^{-1}$ have been achieved in Li–Ni codoped ZnO thin film. Photo-Hall measurements clearly confirm the stability of the Li–Ni-codoped p-ZnO thin film with UV irradiation. The low resistivity and p-type conduction in Li–Ni-codoped ZnO thin film could be attributed to the presence of Ni^{3+} defects, which act as a reactive donors by forming acceptor–donor–acceptor complexes with Li^+ defects and increases Li solubility limit. In addition to optoelectronic applications, this system may find potential applications in spintronics.

AUTHOR INFORMATION

Corresponding Author

*E-mail: msrrao@iitm.ac.in. Phone: +914422574872. Fax: +914422574852.

ACKNOWLEDGMENT

The authors acknowledge Department of Science and Technology (DST) of India for the financial support for the “Establishment of Nano Functional Materials Technology Centre” at IIT Madras [Grant SR/NM/NAT/02-2005]. The authors also acknowledge Dr. Sankar Raman, Physical Electronics, USA, for helping with XPS measurements.

REFERENCES

- (1) Zhu, H.; Shan, C. X.; Yao, B.; Li, B. H.; Zhang, J. Y.; Zhang, Z. Z.; Zhao, D. X.; Shen, D. Z.; Fan, X. W.; Lu, Y. M.; Tang, Z. K. *Adv. Mater.* **2009**, *21*, 1613.
- (2) Tsukazaki, A.; Ohtomo, A.; Onuma, T.; Ohtani, M.; Mahino, T.; Sumiya, M.; Ohtani, K.; Chichibu, S. F.; Fuke, S.; Segawa, Y.; Ohno, H.; Koinuma, H.; Kawasaki, M. *Nat. Mater.* **2005**, *4*, 42.
- (3) Lim, J. H.; Kang, C. K.; Kim, K. K.; Park, I. K.; Hwang, D. K.; Park, S. J. *Adv. Mater.* **2006**, *18*, 2720.
- (4) Xi, Y. Y.; Hsu, Y. F.; Djuricic, A. B.; Ng, A. M. C.; Chan, W. K.; Tam, H. L.; Cheah, K. W. *Appl. Phys. Lett.* **2008**, *92*, 113505.
- (5) Kim, K. S.; Lugo, F.; Pearton, S. J.; Norton, D. P.; Wang, Y. L.; Ren, F. *Appl. Phys. Lett.* **2008**, *92*, 112108.
- (6) Xiao, Z. Y.; Liu, Y. C.; Mu, R.; Zhao, D. X.; Zhang, Y. J. *Appl. Phys. Lett.* **2008**, *92*, 052106.
- (7) Dunlop, L.; Kursumovic, A.; MacManus-Driscoll, J. L. *Appl. Phys. Lett.* **2008**, *93*, 172111.
- (8) Allenic, A.; Guo, W.; Chen, Y.; Katz, M. B.; Zhao, G.; Che, Y.; Hu, Z.; Liu, B.; Zhang, S. B.; Pan, X. *Adv. Mater.* **2007**, *19*, 3333.
- (9) Zhang, J. Y.; Jian, L. P.; Hui, S.; Shen, X.; Deng, T. S.; Zhu, K. T.; Zhang, Q. F.; Wu, J. L. *Appl. Phys. Lett.* **2008**, *93*, 021116.

- (10) Duclere, J. R.; Novotny, M.; Meaney, A.; Haire, R. O.; McGlynn, E.; Henry, M. O.; Mosnier, J. P. *Superlattices Microstruct.* **2005**, *38*, 397.
- (11) Jeong, S. H.; Yoo, D. G.; Kim, D. Y.; Lee, N. E.; Boo, J. H. *Thin Solid Films* **2008**, *516*, 6598.
- (12) Shet, S.; Ahn, K. S.; Yan, Y.; Deutsch, T.; Chrustowski, K. M.; Turner, J.; Jassimand, M. A.; Ravindra, N. *J. Appl. Phys.* **2008**, *103*, 073504.
- (13) Mandalapu, L. J.; Xiu, F. X.; Yang, Z.; Zhao, D. T.; Liu, J. L. *Appl. Phys. Lett.* **2006**, *88*, 112108.
- (14) Ryu, Y.; Lee, T. S.; Lubguban, J. A.; White, H. W.; Kim, B. J.; Park, Y. S.; Youn, C. J. *Appl. Phys. Lett.* **2008**, *88*, 241108.
- (15) Hofstetter, D.; Theron, R.; El-Shaer, A. H.; Bakin, A.; Waag, A. *Appl. Phys. Lett.* **2008**, *93*, 101109.
- (16) Park, C. H.; Zhang, S. B.; Wei, S. H. *Phys. Rev. B.* **2002**, *66*, 073202.
- (17) Yamamoto, T.; Yoshida, H. K. *Jpn. J. Appl. Phys.* **1999**, *38*, L166.
- (18) Lee, E. C.; Chang, K. J. *Phys. Rev. B.* **2004**, *70*, 115210.
- (19) Wardle, M. G.; Goss, J. P.; Briddon, P. R. *Phys. Rev. B.* **2005**, *71*, 155205.
- (20) Zeng, Y. J.; Ye, Z. Z.; Xu, W. Z.; Li, D. Y.; Lu, J. G.; Zhu, L. P.; Zhao, B. H. *Appl. Phys. Lett.* **2006**, *88*, 062107.
- (21) Lu, J. G.; Zhang, Y. Z.; Ye, Z. Z.; Zhu, L. P.; Wang, L.; Zhao, B. H.; Liang, Q. L. *Appl. Phys. Lett.* **2006**, *88*, 222114.
- (22) Singh, S.; Rama, N.; Ramachandra Rao, M. S. *Appl. Phys. Lett.* **2006**, *88*, 222111.
- (23) Jayakumar, O. D.; Gopalakrishnan, I. K.; Kulshreshtha, S. K. *Adv. Mater.* **2006**, *18*, 1857.
- (24) Pei, G.; Xia, C.; Wu, B.; Wang, T.; Zhang, L.; Dong, Y.; Xu, J. *Comput. Mater. Sci.* **2008**, *43*, 489.
- (25) Bian, J. M.; Li, X. M.; Gao, X. D.; Yu, W.; Chen, L. D. *Appl. Phys. Lett.* **2004**, *84*, 541.
- (26) Zhuge, F.; Zhu, L. P.; Ye, Z. Z.; Ma, D. W.; Lu, J. G.; Huang, J. Y.; Wang, F. Z.; Ji, Z. G.; Zhang, S. B. *Appl. Phys. Lett.* **2005**, *84*, 092103.
- (27) Abernathy, C. R.; Mackenzie, J. D.; Pearson, S. J.; Hobson, W. S. *Appl. Phys. Lett.* **1995**, *66*, 1969.
- (28) Brandt, O.; Yang, H.; Kostial, H.; Ploog, K. H. *Appl. Phys. Lett.* **1996**, *69*, 2707.
- (29) Samantha, K.; Bhattacharya, P.; Katiyar, R. S. *J. Appl. Phys.* **2010**, *108*, 113501.
- (30) Wang, B.; Min, J.; Zhao, Y.; Sang, W.; Wang, C. *Appl. Phys. Lett.* **2009**, *94*, 192101.
- (31) Yao, B.; Guan, L. X.; Xing, G. Z.; Zhang, Z. Z.; Li, B. H.; Wei, Z. P.; Wang, X. H.; Cong, C. X.; Xie, Y. P.; Lu, Y. M.; Zhen, D. Z. *J. Lumin.* **2007**, *122–123*, 191.
- (32) Look, D. C.; Calfin, B.; Alivov, Y. I.; Park, S. J. *Phys. Status Solidi A* **2004**, *201*, 2203.
- (33) Petit, L.; Schulthess, T. C.; Svane, A.; Szotek, Z.; Temmerman, W. M.; Janotti, A. *Phys. Rev. B* **2006**, *73*, 045107.

NOTE ADDED AFTER ASAP PUBLICATION

This paper was published on the Web on May 31, 2011. The artwork for the Abstract and Figure 7 were revised and the corrected version was reposted on June 22, 2011.